Hindawi
Advances in Civil Engineering
Volume 2018, Article ID 3410146, 12 pages
https://doi.org/10.1155/2018/3410146

Research Article

Probabilistic Prediction of Maximum Tensile Loads in Soil Nails

Yongqiang Hu[1] **and Peiyuan Lin**[2]

[1]*Assistant Professor, School of Civil Engineering, Guangzhou University, Guangzhou, Guangdong 510 006, China*
[2]*Postdoctoral Fellow, Department of Civil Engineering & Ryerson Institute of Infrastructure Innovation, Ryerson University, Toronto, ON, Canada M5B 2K3*

Correspondence should be addressed to Peiyuan Lin; peiyuan.lin@ryerson.ca

Received 21 August 2018; Revised 29 October 2018; Accepted 6 November 2018; Published 22 November 2018

Guest Editor: Haiyun Shi

This paper presents the development of a simplified model for estimation of maximum nail loads during or at completion of construction of soil nail walls. The developed simplified nail load model consists of two multiplicative components: the theoretical nail load and the correction factor. The theoretical nail load is computed as the product of lateral active Earth pressure at nail depth and the nail tributary area. The correction factor is introduced to account for the difference between the theoretical and the measured nail loads. A total of 85 measured nail load data were collected from the literature; out of which, 74 were used to develop a simple formulation for the correction factor, whereas the remaining 11 were used for validation. After the validation, the model was updated using all 85 data. The updated simplified nail load model was demonstrated to be accurate on average (mean of model factor equal to 1), and the spread in prediction quantified as the coefficient of variation of the model factor was about 40%. Here, model factor is the ratio of measured to estimated nail load. The randomness of the model factor was also verified. Finally, the model factor was demonstrated to be a lognormal random variable. The proposed simplified nail load model is beneficial due to its simplicity and quantified model uncertainty; thus it is practically valuable to both direct reliability-based design and load and resistance factor design of soil nail wall internal limit states.

1. Introduction

Estimation of maximum tensile loads for soil nails during or at completion of construction of soil nail walls is of great practical interests to wall design engineers. Due to the nail-soil interactions, tensile loads develop along soil nails as the nailed soil mass deforms. Failures due to nail pullout or yield in tension take place when the maximum tensile load in a nail exceeds its ultimate pullout capacity or yield tensile strength [1].

There have been several models proposed in the literature for estimation of maximum loads of soil nails during or at completion of wall construction. Juran and Elias [2] developed a modified apparent Earth pressure diagram model which was later found to be not practical as the estimated nail loads are very sensitive to input parameters such as soil friction angle and soil cohesion. Juran et al. [3] proposed a kinematical approach to compute nail loads as the wall construction proceeds and validated their approach using one case study. The underlying model uncertainty of the kinematical approach is not reported in the literature. The Federal Highway Administration (FHWA) soil nail wall design manuals [1, 4, 5] provide a simplified model for nail load estimation. Lin et al. [6] evaluated the model uncertainty of the FHWA simplified model using 45 measured maximum nail load data they collected from the literature and concluded that the default FHWA simplified nail load equation is excessively conservative on average and the estimation scatters widely. Moreover, the model factor of the FHWA equation is not a random variable as it is statistically correlated to some of the input parameters and the calculated nail load. Here, model factor is the ratio of measured to calculated nail load. They then modified the FHWA simplified nail load model to improve on-average accuracy, reduce spreads in prediction accuracy, and remove the dependency between model factor and input parameters and calculated nail load. Indeed, the dependency issue has been reported for various geotechnical models, e.g., bearing capacity of foundations [7–9], both pullout capacities and tensile loads of reinforcing elements in reinforced soil walls [6, 10–13], and deflection of cantilever walls [14]. Removal of this type of dependency is important for geotechnical reliability-based

design as emphasized in ISO2394:2015 Annex D [15] and Phoon [16]. Influence of the dependency on reliability analysis outcomes was discussed by Lin and Bathurst [17].

In this study, a total of 85 measured data for maximum nail tensile loads during or at completion of wall construction are first collected from the literature and divided into two data groups. The first data group is used to develop a simplified model for nail load estimation based on the two regression approaches introduced in Dithinde et al. [18]. The developed simplified model is then validated using the other data group. The simplified model proposed by the present study is advantageous when compared to the default and modified FHWA simplified nail load models from the perspectives of number of empirical constants (i.e., two versus three and five), on-average accuracy (i.e., accurate versus conservative), spread in prediction accuracy (i.e., about 40% versus about 45% and 50%), and dependency between model factor and input parameters or computed nail load. Finally, the distribution of the model factor of the proposed equation is also discussed.

2. Formulation of Simplified Model for Calculation of Maximum Nail Loads

A soil nail wall system is typically divided into an active zone and a passive zone by a potential slip surface, as shown in Figure 1. Nails are installed immediately after excavation of each level to provide both pullout resistance against global failure and restraint against lateral deformation of the excavated ground. Tensile loads are then developed along nails mainly due to the frictional interaction between nails and the surrounding soil and the soil-structure interaction between the facing and the soil at nail heads [19]. The lateral Earth pressure (σ_h) acting within a tributary area (S_hS_v) where a soil nail center is carried by that nail. Based on this mechanism, the tensile load in a soil nail can be calculated as follows:

$$T_N = \eta T_t = \eta \sigma_h S_h S_v = \eta K_a (\gamma h + q_s) S_h S_v, \quad (1)$$

where T_t is the theoretical nail load computed as $T_t = \sigma_h S_h S_v = K_a(\gamma h + q_s) S_h S_v$; $\sigma_h = K_a(\gamma h + q_s)$ is the horizontal Earth pressure at depth of nail head h as defined in Figure 1; K_a is the active Earth pressure coefficient computed using Coulomb theory; γ is the soil unit weight; q_s is the surcharge load; S_h and S_v are the horizontal and vertical nail spacing, respectively; and η is the empirical correction factor introduced to account for errors arising from underlying model errors, variability in soil properties, and all types of uncertainties in sites, etc. The Coulomb K_a is computed as follows:

$$K_a = \frac{\cos^2(\beta + \phi)}{\cos^2\beta \cos(\beta - \delta)\left[1 + \sqrt{(\sin(\phi + \delta)\sin(\phi - \alpha))/(\cos(\beta - \delta)\cos(\alpha + \beta))}\right]^2}, \quad (2)$$

where β = face batter angle; ϕ = effective soil friction angle; α = back slope angle; and δ = interface friction angle between the wall face and soil.

The formulation structure of Equation (1) is consistent to those currently used in AASHTO [20] and FHWA [21] for estimation of loads in reinforcing elements such as steel strip, steel grid, and geosynthetic sheet (geogrid or geotextile). The only difference is the expression of the empirical term η which is dependent on the type of reinforcing elements. One of the advantages of Equation (1) is the compatibility in formulation with those for design of different types of reinforced soil walls per AASHTO [20] and FHWA [21]. The remaining of this study is focused on the development of simple expression of η for soil nails.

3. Database of Maximum Soil Nail Loads under Working Conditions

This study developed a large database of measured soil nail loads based on two components. The first is the database that was developed by Lin et al. [6] (walls W1 to W9 in Table 1), and the second is new data that we collected from the literature (walls W10 to W19 in Table 1). Summary of the wall geometry, soil type and properties, nail arrangement, and surcharge loading conditions for those soil nail walls are shown in Table 1; while detailed descriptions are provided in the following.

Lin et al. [6] developed a database of measured short-term maximum tensile loads of soil nails. Here, short-term means that the nail loads were recorded during or at completion of wall construction. There were 45 data points from nine soil nail walls included in their database; all the walls were constructed, instrumented, and monitored within the United States for different applications. In Table 1, walls W1 and W2 by Banerjee et al. [22] were nearby each other; W1 was constructed below an existing bridge abutment, whereas W2 was not beneath the bridge abutment but about 15 m to the west. Wall W3 by Shen et al. [23] was a full-scale field prototype built as a part of the systematic studies on in situ Earth retaining structures. Wall W4 by Juran and Elias [2] was featured by both the inclined facing and upper ground back slope. Temporary walls W5 to W7 by Holman and Tuozzolo [24] were used to support the construction of a large electrical vault, for which the site accessibility was very limited in size and the construction schedule was aggressive. Walls W8 and W9 by Wei [25] were from an MSE/soil nail hybrid project where the soil nail walls were sitting beneath the MSE walls for an overpass of a road.

It is noted that for a soil nail, there were several strain gauges mounted along its length, and only the one that gave the maximum nail load was adopted. In the database by Lin et al. [6], the soil nail walls were typically less than 10 m high with horizontal back slope and vertical facing structure. Those walls were built in a wide variety of cohesive and

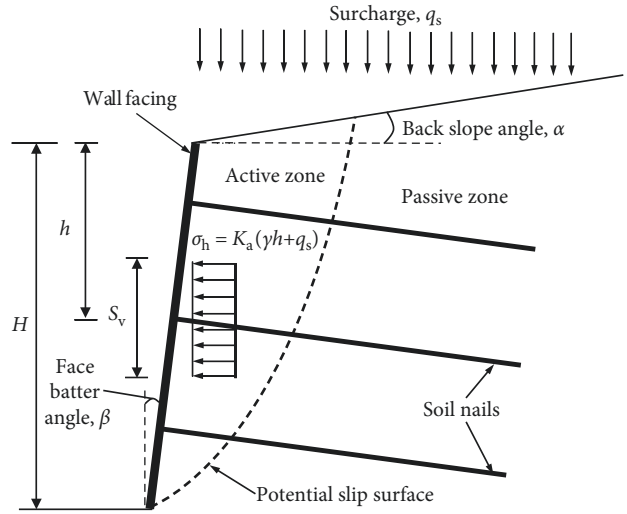

Figure 1: Geometry of soil nail walls and horizontal stress of soil acting on the wall.

Table 1: Summary of wall geometry, soil properties, and nail arrangement for soil nail walls reported in the source documents.

Data group	Wall	Source	Soil	Wall geometry			Surcharge	Soil strength parameters			Nail spacing		No. of data
				H (m)	α (°)	β (°)	q_s (kPa)	ϕ (°)	c (kPa)	γ (kN/m^3)	S_h (m)	S_v (m)	
1	W1	[22]	Medium dense, poorly graded sand	5.3	0	0	55	33	4.8	18.0	1.4	1.0	5
	W2	[22]	Silty sand, clayey silt	5.6	0	27	0	33	4.8	18.0	1.4	1.0	5
	W3	[23]	Heterogeneous SM	9.2	0	0	0	36.5	18.5	16.3	1.85	1.85	3
	W4	[2]	Residual soil and weathered rock	9–12	16	25	0	38	7.2	18.9	1.5	1.5	7
	W5	[24]	Fill, silt, sand	7.6	0	0	0	38	0	19.6	1.83	1.22–1.83	4
	W6	[24]	Fill, silt, sand	5.9	0	0	0	38	0	19.6	1.83	1.22–1.52	3
	W7	[24]	Fill, silt, sand	5.9	0	0	0	38	0	19.6	1.83	1.22–1.52	3
	W8	[25]	Gravelly silty sand	4-5	0	0	0–127	35	0	19.6	1.0	1.05	3
	W9	[25]	Gravelly silty sand	4-5	0	0	0–127	35	0	19.6	1.0	1.05	12
	W10	[26]	Silty clay	9.2	8.5	0	0	10	0	19.6	1.5	1.5	4
	W11	[27]	Silty sand, fine sand	10	0	0	35	30.6	0	19.1	1	1–1.2	3
	W12	[28]	Clay, silty clay	12	0	0	15	16–20	16–18	19	1.5	1.5	4
	W13	[29]	Silty clay	8	0	0	0	16.4	12	19.7	1.2	1.2	6
	W14	[30]	Sand	6	11.3	0	0	35	0	21	1.5	1.5	4
	W15	[31]	Silty clay	8.5	11.3	0	0	18.9	21	19.8	1.5	1.5	5
	W16	[31]	Silty clay	8.5	15.8	0	0	18.9	21	19.8	1.5	1.5	3
2	W17	[32]	Sand	6	12	0	16	33	0	16	1.25	1.46	4
	W18	[33]	Clayey or silty gravel	5.8–10.6	30	0	0	27	3	18	1.7, 1.8	1.2, 2.1	7
	W19	[34]	Residual andesite	10	0	0	0	38	0	19	2.0	1.5	1

noncohesive soils, including sand, silty sand, clayey silt, residual soil, and weather rock. Despite various soil types, the soil friction angles varied in a relatively narrow rages, i.e., from 33° to 38°. Three walls were surcharged with an equivalent soil height less than 6 m; the majority were under self-weight-loading conditions.

In this study, by surveying the literature, we expanded their database to include another 40 data points from ten soil nail walls (i.e., walls W10 to W19 in Table 1), resulting in a larger database that includes a total of 85 short-term nail load data. Importantly, these additional data were collected from soil nail walls built in the United States, China, Poland, and South Africa. Therefore, the larger database developed in this study is more international. Walls W10 to W16 were soil nail walls built in China mainly for support of foundation pits for high-rise buildings (i.e., [26, 28–31]), except for W11 by Duan et al. [27] for supporting excavation in a tunnel project. Wall W17 by Sawicki et al. [32] was the first wall built in Poland to protect and strengthen a steep slope of an excavation in loose sandy subsoil. Wall W18 by Turner and Jensen [33] was from an MSE/soil nail wall hybrid project in the United States aiming at demonstrating the feasibility of using soil nails for stabilization of active landslides. Wall 19 by Jacobsz and Phalanndwa [34] was used to support an excavation for a railway line in South Africa.

The newly added data were from soil nail walls that were typically built in clayey silt and sand. In general, the friction angles varied widely, i.e., from 10° to 38° but typically less than 30°. The wall heights were from about 6 m to 12 m, which were typical. All the walls had horizontal back slopes while most had inclined facing. The walls were typically subjected to self-weight loads.

By examining the source documents carefully, we found that two maximum load measurements in Turner and Jensen [33] were anomalously large compared to other measurements in the same nails. The strain gauges giving these two large nail loads were mounted near the facing, leading to the possibility that the anomalously large measurements could have been due to the bending of the nails due to the facing installation. As a result, these two questionable data were not adopted; instead, the second largest measurements in the same nails were adopted.

In addition, the source documents do not specify whether or not the strain gauge measurements had been calibrated against temperature. Hence, the effect of temperature is not considered in the development of the simplified nail load model in this study. It is also revealed that some source documents also reported long-term nail loads which were recorded several years after completion of wall construction. However, since this study is exclusively focused on prediction of short-term nail loads, those long-term data are thus not included in the analyses to follow.

The larger database ($n = 85$) developed in this study are divided into two data groups: a verification group (group 1) and a validation group (group 2). The verification group contains 74 data and is used to determine the η expressions for the simplified nail load estimation model. Then, the developed simplified nail load model is validated using the validation group, which contains 11 data points. After the validation, the empirical constants appearing in the simplified model are updated using all collected data (i.e., data groups 1 and 2). This final updated simplified model is the model that is proposed by the present study. The model factor of this final updated model is then characterized.

Last, it should be pointed out that the importance of compiling a larger database for model evaluation and calibration should not be undervalued. The number of data points in the present database is almost doubled compared to the previous one by [6]. It contains nail load data from wider working conditions. When a model is scrutinized within a larger context, the merits and demerits of the model can be seen more clearly. From a statistical and also practical point of view, a larger database is desirable as it provides more confidence on the quantitative model estimation and calibration outcomes.

4. Formulation of the Empirical Correction Term η

Dithinde et al. [18] summarize two regression approaches that are widely used in the literature for determination of η. The first approach is the generalized model factor framework which regresses measured nail loads against theoretical values, and η is a function of T_t expressed as $\eta = f(T_t)$. The second approach is to regress measured nail loads against each input parameter of T_t, and η is expressed as $\eta = f(K_a) \times f(\gamma) \times f(h) \times f(q_s) \times f(S_h S_v)$. Both approaches are adopted for determination of η in Equation (1).

4.1. Generalized Model Factor Approach. The parameter δ in Equation (2) must be specified before further analyses can be carried out. The range of ratio of δ to ϕ is commonly assumed to be from 1/2 to 2/3 for different types of retaining walls (e.g., [35]). Based on this range, $\delta/\phi = 1/2$ is first selected in this study for analysis while the justification is presented later.

As the nail load data were collected from soil nail walls under different working conditions, for example, some data were from nails in hybrid soil-nail/MSE walls while others were not; it should first check that whether or not the formulation of η depends significantly on the wall-working conditions. To do the check, this study divides the verification data group ($n = 74$) into different data subsets based on three criteria: (1) data from hybrid walls or pure soil nail walls; (2) data from soil nail walls with or without surcharge; and (3) data from walls in cohesive or cohesionless soils. Ideally, the data should be grouped concurrently according to these three criteria; however, as there are only 74 data in total, such a detailed data-grouping approach would make each individual data subset very small, i.e., on average less than 10 points. As a result, this study groups the data based on one criterion at one time. That being said, the 74 data are divided into two data subsets, corresponding to either criterion 1, or 2, or 3.

With measured nail loads T_m, the measured empirical correction factors can be computed as $\eta = T_m/T_t$, where $T_t = K_a(\gamma h + q_s)S_h S_v$ is theoretical nail load as defined in Equation (1). By using the generalized model factor approach, in this study, η is regressed against $T_t/P_a/A_t$, where $P_a = 101$ kPa is the atmospheric pressure and $A_t = 1.5 \times 1.5\,\text{m}^2 = 2.25\,\text{m}^2$ the is typical nail tributary area computed using typical horizontal and vertical nail spacing of 1.5 m [6]. The introduction of P_a and A_t is for normalization of T_t and makes it dimensionless. Figure 2 shows the plots of η versus $T_t/P_a/A_t$ with respect to different data subsets for soil nail walls under different working conditions.

The first observation from Figure 2 is that the measured η values in general decrease monotonically (at least visually) and nonlinearly with increasing $T_t/P_a/A_t$ values. The measured η is more likely to be larger than 1 for $T_t/P_a/A_t < 0.1$, meaning that the true nail load is more likely to be underestimated if taken as T_t. For larger $T_t/P_a/A_t$ values, e.g., >0.2, the true nail load is more frequently overpredicted if taken as T_t since the η value is much likely smaller than 1. The second observation is that the overall trend between η and $T_t/P_a/A_t$ holds regardless of wall-working conditions, i.e., nails in pure soil nail walls or in hybrid walls, walls with or without surcharge, and walls in cohesive and cohesionless soils. Hence, in the following analyses for the formulations for $\eta = f(T_t/P_a/A_t)$, all the measured data ($n = 74$) will be used.

Various formulations could be proposed for η, e.g., nonmonotonic, higher-order functions. Sophisticated

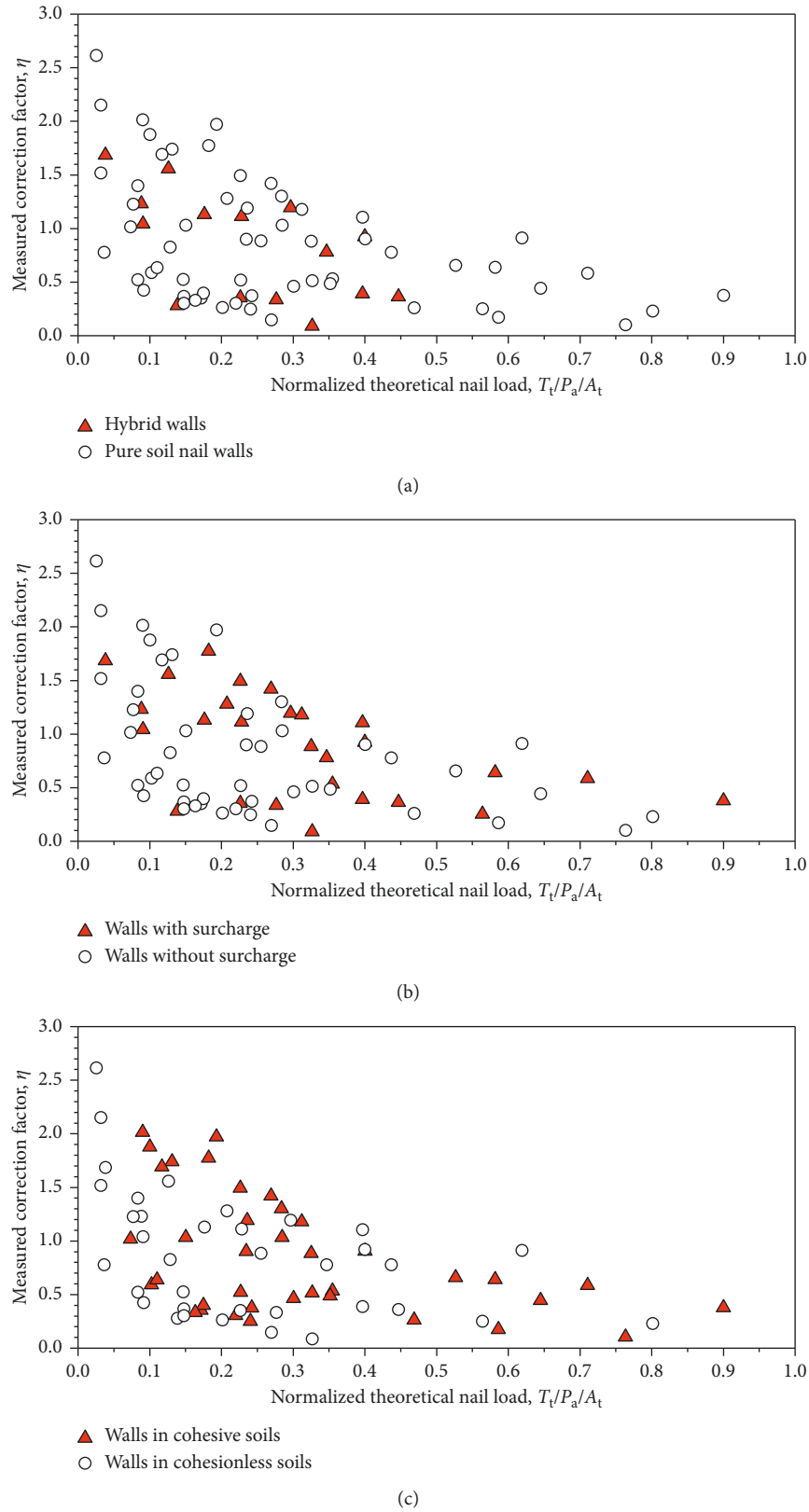

FIGURE 2: Measured correction factor η versus normalized theoretical nail load $T_t/P_a/A_t$ for different data subsets grouped based on soil nail wall-working conditions.

functions, although might fit the data better, are undesirable due to the complexity. In addition, they could result in overfitting issues. This study advocates the adoption of simple formulations for practical purpose. Therefore, four simple candidate expressions were examined, including exponential, linear, logarithmic, and power functions. The four expressions can be written as follows:

$$\eta = a \times \exp\left(b \times T_t/P_a/A_t\right), \quad \text{exponential,} \tag{3a}$$

$$\eta = a \times \left(T_t/P_a/A_t\right) + b, \quad \text{linear,} \tag{3b}$$

$$\eta = a \times \ln\left(T_t/P_a/A_t\right) + b, \quad \text{logarithmic,} \tag{3c}$$

$$\eta = a \times \left(T_t/P_a/A_t\right)^b, \quad \text{power,} \tag{3d}$$

where a and b are the empirical constants to be determined. The determination of a and b must satisfy three criteria: (1) the mean of model factor, μ_M, for Equation (1) should be equal to one; (2) the COV of model factor, COV_M, should be as small as possible; and (3) the model factor, M, should be a random variable, which means that M is not statistically correlated to any input parameters or the calculated T_N values using Equation (1).

The steps to determine the optimal values of a and b are as follows: (1) select an expression for η (e.g., Equation (3a)) and substitute into Equation (1); (2) compute model factors as $M = T_m/T_N$ where T_m are the measured nail load values and T_N are matching calculated values using Equation (1); and (3) determine the values of a and b as the pair that minimizes COV_M (Criterion 2) while keeps $\mu_M = 1.00$ (Criterion 1).

Table 2 summarizes the analysis outcomes using the generalized model factor framework and data group 1 ($n = 74$). The minimal COV_M was 0.535 corresponding to η being a power function of T_t (Equation (3d)) with $a = 0.34$ and $b = -0.47$. To verify the randomness of M for this case, Spearman's rank correlation test was applied to M against T_N which gave the p value of 0.54 (>0.05), indicating rejection of the null hypothesis that the two datasets are statistically correlated at a level of significance of 5%. Further examinations showed that there is correlation at a level of significance of 5% between M and the nail depth h. This independency between M and h was doubly confirmed by the outcome of Pearson's correlation test. Hence, the calibrated η expression in this case is judged to be unsatisfactory.

For η with other formulations (i.e., exponential, linear, and logarithmic), the COV_M values for Equation (1) are all higher, and M is also correlated to h for all the three cases. This suggests inadequacy for calibrating η to the level of T_t as the generalized model framework provides no physical insight on the sources of statistical correlations [18]. Calibration to the level of each input parameter is needed.

4.2. Correction Term η as a Function of Input Parameters. This approach assumes that η is a function of input parameters of Equation (1) and can be generally expressed as $\eta = f(K_a) \times f(\gamma) \times f(h) \times f(q_s) \times f(S_h S_v)$. The formulation of η could be too complicated to be practical if all the input parameters are taken into account. A common strategy to simplify the formulation of η is to identify and address the most important influential factors, while ignoring those that are of secondary significance. This can be easily done by carrying out correlation tests between measured η values and values of input parameters. Note that the measured η value is computed as T_m/T_t based on Equation (1) where T_m is the measured nail load and $T_t = K_a(\gamma h + q_s)S_h S_v$ is the theoretical value as defined earlier in this paper.

Table 3 shows the ρ and p values between η and each input parameter using both Spearman's rank and Pearson's correlation tests. It appears that the measured η values are strongly correlated to the depths of nail head h, but independent of K_a, q_s, and $S_h S_v$ at the level of significance of 5%. For the soil unit weight, γ, the p value from Spearman's rank test was 0.04, slightly lower than 0.05, suggesting a correlation between η and γ. On the contrary, Pearson's correlation test result suggested the opposite, p value = 0.32 (far exceed 0.05). To further investigate whether or not γ should be formulated into η, the four simple expressions adopted earlier were used to fit η against γ, and the coefficients of determination (R^2) were computed. The results showed that the R^2 values were 0.015, 0.014, 0.011, and 0.012 for exponential, linear, logarithmic, and power functions of $\eta = f(\gamma)$, respectively. These R^2 values were very small, indicating that including γ into the formulation of η is reluctant to improve the accuracy at a noticeable extent. Moreover, in reality, the unit weight of soils that are suitable for soil nailing applications usually varies in a relative small range. As a result, in this study, the formulation of η was greatly simplified to be as $\eta = f(h/H)$. The introduction of wall height H is intended to make η dimensionless. It should be pointed out that this is a different normalization treatment from that for the first case as in the first case, P_a and A_t are both constants regardless of walls, whereas in this second case, H varies from one wall to another. Expectedly, different normalization strategies could result in different calibration outcomes; nevertheless, the differences are insignificant and thus not quantitatively analyzed here.

Figure 3 shows the plot of measured η values (T_m/T_t) versus normalized depths (h/H) using data subsets grouped based on wall-working conditions as defined earlier. The measured η appears to decrease monotonically with increasing h/H. The trend differentiates insignificantly among different wall-working conditions. Hence, further analyses are based on all data points ($n = 74$).

It has been shown, e.g., [1, 5, 6], that T_m typically increases with h/H within the upper quarter of wall height and roughly keeps constant before h/H reaching about 0.7-0.8, then decreases with larger h/H until at round zero at the bottom of the wall. While for T_t, it increases monotonically with increasing h/H. They together result in the decreasing of measured η values against increasing h/H. On average, the measured η values are greater than 1.0 within $h/H = 0$ and about $h/H = 0.50$, suggesting underestimation of nail loads if taken as T_t. For greater depth (i.e., $h/H > 0.50$), nail loads would generally be overestimated if taken as T_t. The reason for this is that the nail load data were collected from soil nail walls built following the top-down construction procedure,

Table 2: Calibration outcomes based on both $\eta = f(T_t/P_a/A_t)$ and $\eta = f(h/H)$ using data group 1 ($n = 74$).

Case	Simple formulation		Constants		Model factor, M		Spearman's p value between model factor M and						
	Name	Expression*	a	b	μ_M	COV_M	η	K_a	γ	h	q_s	S_hS_v	T_N
Generalized model factor approach	Exponential	$\eta = a \times \exp(b \times T_t/P_a/A_t)$	1.19	−1.77	1.00	0.558	0.09	0.20	0.08	0.00	0.47	0.89	0.06
	Linear	$\eta = a \times (T_t/P_a/A_t) + b$	−0.92	1.05	1.00	0.580	0.01	0.45	0.11	000	0.44	0.90	0.00
	Logarithmic	$\eta = a \times \ln(T_t/P_a/A_t) + b$	−0.33	0.26	1.00	0.538	0.23	0.14	0.11	0.00	0.36	0.91	0.23
	Power	$\eta = a \times [T_t/P_a/A_t]^b$	0.34	−0.47	1.00	0.535	0.54	0.09	0.13	0.00	0.32	0.98	0.54
Calibration to h/H	Exponential	$\eta = a \times \exp(b \times h/H)$	2.05	−2.11	1.00	0.439	0.18	0.64	0.12	0.15	0.18	0.04	0.27
	Linear	$\eta = a \times (h/H) + b$	**−1.45**	**1.53**	**1.00**	**0.424**	**0.25**	**0.34**	**0.08**	**0.13**	**0.16**	**0.05**	**0.06**
	Logarithmic	$\eta = a \times \ln(h/H) + b$	−0.71	0.20	1.00	0.434	0.52	0.77	0.10	0.42	0.16	0.03	0.33
	Power	$\eta = a \times (h/H)^b$	0.39	−0.72	1.00	0.474	0.01	1.00	0.07	0.01	0.19	0.04	0.23

Note: *P_a (101 kPa) is the atmospheric pressure, and A_t (1.5 m × 1.5 m = 2.25 m^2) is the typical tributary area. They are introduced to make the empirical correction term η dimensionless.

Table 3: Outcomes of correlation tests between measured η values and values of input parameters based on data group 1 ($n = 74$).

Input parameter	Spearman's rank correlation test		Pearson's correlation test	
	ρ	p value	ρ	p value
Coulomb Earth pressure coefficient, K_a	−0.09	0.43 > 0.05	−0.20	0.09 > 0.05
Soil unit weight, γ	−0.24	0.04 < 0.05	−0.12	0.32 > 0.05
Depth of nail head, h	**−0.71**	**0.00 < 0.05**	**−0.64**	**0.00 < 0.05**
Surcharge, q_s	0.07	0.54 > 0.05	0.02	0.88 > 0.05
Tributary area, S_hS_v	−0.10	0.38 > 0.05	−0.03	0.80 > 0.05

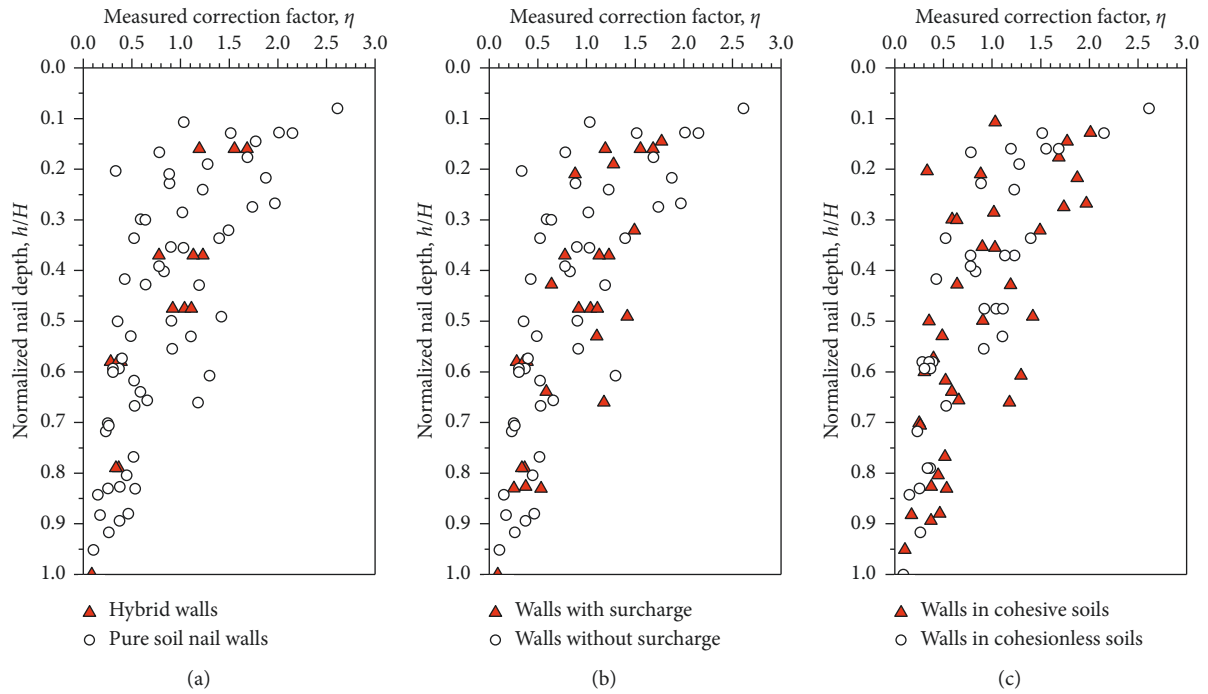

Figure 3: Measured correction factor η versus normalized nail depth h/H for different data subsets grouped based on soil nail wall-working conditions.

which resulted in larger lateral deformations and hence more mobilization of nail tensile loads at shallower depth (i.e., closer to the top of the walls).

Again, the four simple expressions were adopted, i.e., exponential, linear, logarithmic, and power functions. Steps to determine the formulation of $\eta = f(h/H)$ are similar to those for $\eta = f(T_t/P_a/A_t)$. Calibration outcomes using data group 1 ($n = 74$) are summarized in Table 2. The smallest COV_M is achieved as 0.424 when η is a linear function of h/H. Spearman's rank correlation test outcomes showed that, in this case, the model factor M is not correlated to T_N and any input parameters at a level of significance of 5%. Therefore, the calibration outcomes are satisfactory.

Figure 4(a) shows the plots of measured versus computed nail loads using Equation (1) with $\eta = a \times (h/H) + b$ and $a = -1.45$ and $b = 1.53$ (from Table 2). The majority of the data points scatter within $M = T_m/T_N = 0.5$ and 2. The causes of deviation of data points from the line of $T_m/T_N = 1$ include the randomness and spatial variability of soil properties, variation in time to record the strain gauge readings, systematic errors in conversion from strain gauge readings to nail loads, and underlying model errors of Equation (1), as explained in [6]. Figure 4(b) shows the plots of model factors against computed nail loads, and expectedly, there is no visual trend between M and T_N as the p value is larger than 0.05.

Based on Table 2, taking the correction term η in Equation (1) as a linear function of h/H gives the best outcomes in terms of COV_M. As such, Equation (1) is now expressed as follows:

$$T_N = \left(a \times \left(\frac{h}{H}\right) + b\right) K_a (\gamma h + q_s) S_h S_v, \tag{4}$$

where $a = -1.45$ and $b = 1.53$ based on data group 1.

4.3. Validation and Update of the Developed Simplified Nail Load Model. The measured nail loads in data group 2 are plotted against the corresponding computed nail loads using Equation (4) with $a = -1.45$ and $b = 1.53$, as shown in Figure 4(a). The data points basically fall between $M = 0.5$ and $M = 1.5$. Based on data group 2, the model factor of Equation (4) is found to have a mean of $\mu_M = 1.19$ with a COV of $\mathrm{COV}_M = 0.325$. These values are comparable to those using data group 1, which are 1.00 and 0.424, respectively. A two-sample Kolmogorov–Smirnov test was applied to the two model factor datasets. The results showed that the two distributions are not significantly different at a level of significance of 0.05. Furthermore, Spearman's rank correlation test is applied to the computed model factors against the computed nail loads, giving Spearman's $\rho = -0.25$ and p value = 0.47 > 0.05 as shown in Figure 4(b). The correctness of Equation (4) is thus demonstrated.

Data group 2 is now merged into data group 1 to form a larger data group ($n = 74 + 11 = 85$). This larger data group is then used to update the empirical constants a and b in Equation (4). The final optimal values are $a = -1.45$ and $b = 1.55$ after rounded up to two decimal places, which are very close to those previously determined based on data group 1. The corresponding mean and COV of the model factor are $\mu_M = 1.00$ and $\mathrm{COV}_M = 0.412$. No dependencies between M and T_N or any input parameters are detected. Equation (4) with $a = -1.45$ and $b = 1.55$ is the proposed simplified nail load model in the present study.

4.4. Influence of Ratio of δ/ϕ on η. The ratio of friction angle at facing-soil interface (δ) and soil friction angle (ϕ) was taken as 1/2 in the analyses presented above. The influence of ratio of δ/ϕ on the calibration outcomes is examined using all data groups. Figure 5 shows that as the δ/ϕ ratio increases from 0 to 1.0, the minimal COV_M decreases from 0.419 to 0.403, given μ_M is maintained at 1.00. The reduction is even smaller within the typical range of interest, i.e., δ/ϕ from 1/2 to 2/3. From a practical point of view, the influence of δ/ϕ on the minimal COV_M value is judged to be negligible. Hence, using $\delta/\phi = 1/2$ in the previous analyses is justified.

4.5. Characterization of Distribution of Model Factor. The model uncertainty of Equation (4) with $a = -1.45$ and $b = 1.55$ for estimation of nail loads was shown to have $\mu_M = 1.00$ and $\mathrm{COV}_M = 0.412$. Figure 6 shows the cumulative distribution function plot of the model factors. The vertical axis is the standard normal variable, z. The horizontal axis is in log scale.

Visually, a first-order polynomial seems adequate to capture the overall data trend. This is quantitatively confirmed by the outcomes of Kolmogorov–Smirnov (K-S) test that was applied to the logarithm of the model factor (M) values. The K-S test results suggested that the logarithm of the M values can be considered to be significantly drawn from normally distributed populations. This means that M can be taken as a lognormal random variable. The K-S test was also applied directly to the M values, which suggested that M can also be taken as a normal random variable. However, the main disadvantage of using normal distribution model is that negative M values could be generated using the Monte Carlo simulation technique, which is physically impossible based on the definition of M (i.e., measured to computed nail load). From this perspective, model factor M is always considered lognormally distributed in the literature (e.g., [36–38]). Cautions are required when taking M as a normal random variable in reliability-based design or calibration of resistance factors for load and resistance factor design methods.

5. Comparisons to Default and Modified FHWA Simplified Nail Load Models

The default FHWA simplified model to estimate maximum loads in soil nails is based on an empirical trapezoid envelope roughly fitted to the data collected by Banerjee et al. [22]. The model equation is written as follows [1, 4, 5]:

$$T_N = \eta K_a (\gamma H + q_s) S_h S_v. \tag{5}$$

Parameters in the equation are as defined earlier in this paper. Equations (4) and (5) are similar in formulation but there are two differences. First, the height of wall, H, is used in Equation (5), while for Equation (4), the depth of nail head, h, is used. Second, the expression of the empirical correction term, η, is different. η for the default FHWA simplified model is a piecewise function of h/H expressed as follows:

$$\eta = \begin{cases} a \times \left(\dfrac{h}{H}\right) + b, & \text{for } 0 < \left(\dfrac{h}{H}\right) \le 0.2, \\ c, & \text{for } 0.2 < \left(\dfrac{h}{H}\right) \le 0.7, \text{ and} \\ d - e \times (h/H), & \text{for } 0.7 < \left(\dfrac{h}{H}\right) \le 1, \end{cases} \tag{6}$$

where the function η contains a total of five empirical constants, including $a = 1.25$, $b = 0.50$, $c = 0.75$, $d = 2.03$, and

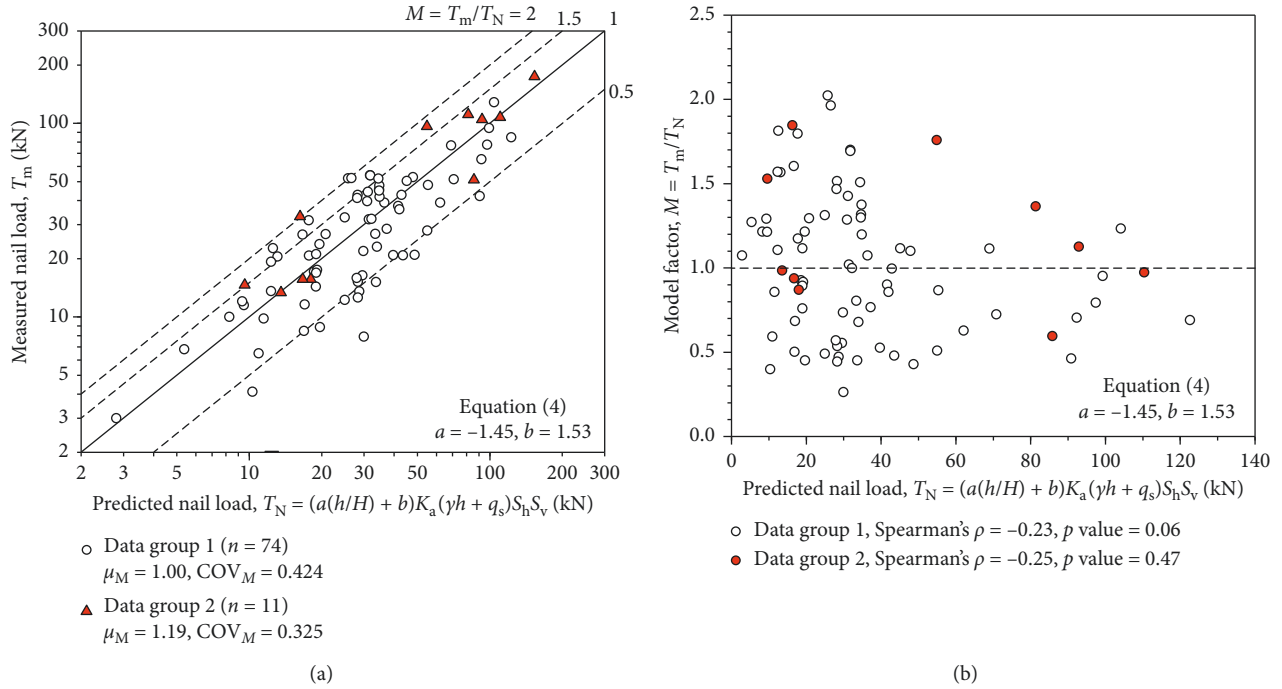

FIGURE 4: Analyses of Equation (4) using different data groups: (a) measured versus calculated nail load; (b) model factor versus calculated nail load.

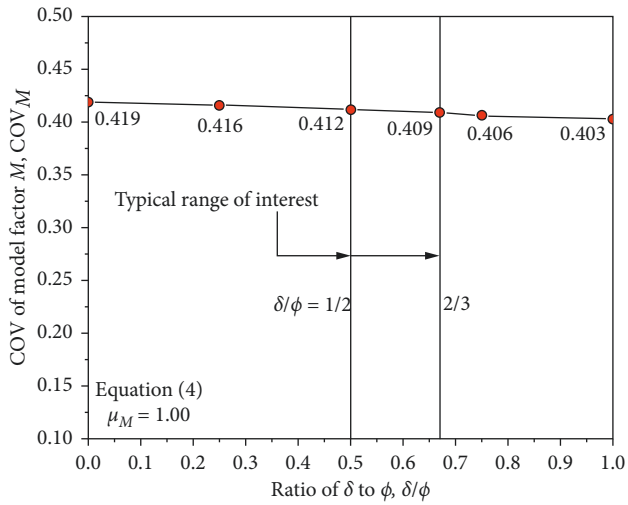

FIGURE 5: Influence of ratio of δ to ϕ on optimization outcomes of COV of model factor (COV_M) for Equation (4).

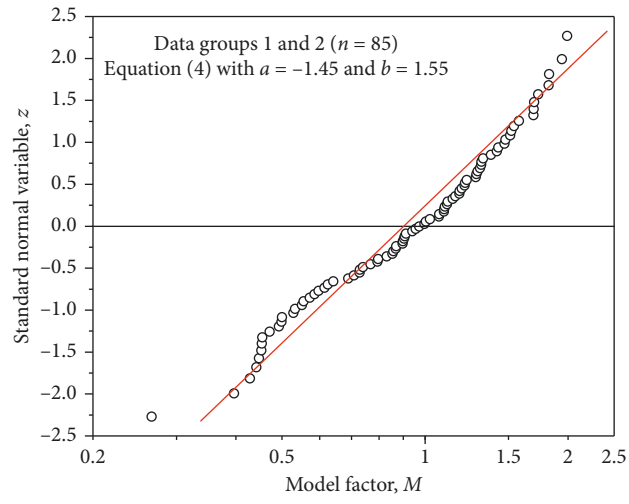

FIGURE 6: Cumulative distribution function plots of model factor of Equation (4) using all nail load data ($a = -1.45$; $b = 1.55$).

$e = -1.83$. The model uncertainty of the default FHWA simplified model was evaluated by [6]. They concluded that the performance of Equation (5) jointly with Equation (7) is unsatisfactory, and then they modified the expression of η for accuracy improvement as follows:

$$\eta = \left[\frac{S_h S_v}{A_t}\right]^a \times \left[-\left(\frac{h}{H}\right)^2 + b\left(\frac{h}{H}\right) + c\right]. \quad (7)$$

The number of empirical constants were reduced to three, i.e., a, b, and c. The values of the empirical constants are $a = -0.67$, $b = 0.84$, and $c = 0.25$ for nails during or at completion of wall construction. Equation (5) jointly with Equation (7) is called modified FHWA simplified nail load estimation model in this paper.

The empirical constants a, b, and c in Equation (7) were calibrated using a subset of the database presented in this study, i.e., $n = 45$ [6]. Now the total number of data points has been expanded to 85. To allow a fair comparison, Equation (7) was recalibrated using the present expanded database. The optimal set of a, b, and c values was computed as $a = 0.04$, $b = -0.14$, and $c = 1.20$, after rounded to two decimal places. The model factor of the modified FHWA simplified nail load equation was then reestimated. After

Table 4: Comparisons of model accuracy in estimation of maximum nail loads among different models.

Method	Model equation	Empirical term, η^*	Empirical constants					μ_M^{**}	COV_M^{**}	M correlated to	
			a	b	c	d	e			T_N	Input para.
The present study	$T_N = \eta K_a(\gamma h + q_s)S_h S_v$	$\eta = a \times (h/H) + b$	−1.45	1.55	—	—	—	1.00	0.412	No	None
Default FHWA simplified model	$T_N = \eta K_a(\gamma h + q_s)S_h S_v$	(1) $\eta = a \times (h/H) + b$, if $0 < h/H \le 0.2$, (2) $\eta = c$, if $0.2 < h/H \le 0.7$, (3) $\eta = d - e \times h/H$, if $0.7 < h/H \le 1$.	1.25	0.50	0.75	2.03	−1.83	0.59	0.516	Yes	$S_h S_v$, K_a
Modified FHWA simplified model	$T_N = \eta K_a(\gamma h + q_s)S_h S_v$	$\eta = [(S_h S_v)/A_t]^a \times [-(h/H)^2 + b(h/H) + c]$	0.04	−0.14	1.20	—	—	1.00	0.454	No	None

Note: $^*A_t$ (1.5 m × 1.5 m = 2.25 m^2) is the typical tributary area; **based on both data groups, i.e., data groups 1 and 2 (n = 85).

recalibration, the model factor of the modified FHWA simplified model has a mean of 1.00 and a COV of 0.454.

A comparison of model uncertainty of each nail load estimation model using all data groups is presented in Table 4. The default FHWA simplified model is excessively conservative since on average it overestimates the maximum nail loads by about 40%. The spread in prediction quantified as COV_M is over 50%. Moreover, the model factor of the default FHWA simplified model is statistically correlated to calculated T_N values and input parameters of $S_h S_v$ and K_a. All these suggest unsatisfactory performance of the default FHWA simplified model in prediction of nail loads during or at completion of wall construction. While for the recalibrated modified FHWA simplified model and the simplified model proposed by the present study, based on the collected data (i.e., data groups 1 and 2), both models are much better than the default FHWA model as they are accurate on average, and the dependency issue of the model factors is not present. Nonetheless, the present model is more advantageous as it has less scatter in prediction, i.e., COV_M = 0.412 for the present model versus COV_M = 0.454 for the recalibrated modified FHWA model. Last, the present model has only two empirical constants, compared to five and three for the default and modified FHWA simplified models, respectively.

6. Concluding Remarks

A simplified model for estimation of maximum tensile loads for soil nails during or at completion of wall construction is developed in this study based on a total of 85 measured data collected from instrumented soil nail walls reported in the literature. The formulation of the developed simplified model has two multiplicative components: one is the theoretical nail loads expressed as the product of lateral active Earth pressure at depth of the nail head and the tributary area where the nail head centers; the other is a simple correction term (function) with two empirical constants introduced for improvement of estimation accuracy. The 85 collected measured nail load data are divided into two data groups. Data group 1 is used to determine the optimal values of the two empirical constants in the simple correction term using both the generalized model factor framework approach and the approach of model factor as a function of input parameters introduced in Dithinde et al. [18]. Here, model factor is defined as the ratio of measured to calculated nail load. Then the developed simplified nail load model is validated using data group 2. After validation, the two data groups are merged into one larger dataset and used to update the values of the two empirical constants in the proposed simplified nail load equation.

Based on the collected nail load data, the model factor of the developed simplified nail load estimation equation has a mean of 1.00 and a COV of about 40%. Moreover, the model factor is not statistically correlated to the magnitude of the calculated nail load or any input parameters of the proposed nail load equation. In addition, there are less empirical constants in the present simplified nail load model equation compared to the default and modified FHWA simplified models [1, 4–6], i.e., the number of empirical constants is two versus five and three. Finally, the model factor of the proposed simplified model is characterized as a lognormal random variable based on the result of the Kolmogorov–Smirnov test.

The simplified nail load model developed in this study is compatible with the current soil nail wall design framework proposed in the FHWA soil nail wall design manual [1]. Also, the model uncertainty of the simplified model has been quantified and therefore the model is practically valuable to both direct reliability-based design and load and resistance factor design (LRFD) of internal limit states of soil nail walls, i.e., nail pullout limit state and nail tensile yield strength limit state.

Last, it is reminded that design methodologies, construction techniques, and site conditions differ from one soil nail wall project to another. Hence, the nail load database developed in this study should be taken as a "general" database. The proposed model based on such a database does not necessarily apply to any specific soil nail wall projects. In practice, design engineers must review and compare all the conditions against those specified in the present database and utilize their expertise to judge the suitability of the proposed default model. Moreover, for cases where project-specific nail load data are available, the Bayesian updating approaches (e.g., [39–41]) can be employed to refine the proposed default model to reflecting the specific site conditions of the projects.

Data Availability

The data used to support the findings of this study are available from the corresponding author upon request.

Conflicts of Interest

The authors declare that they have no conflicts of interest.

References

[1] C. A. Lazarte, H. Robinson, J. E. Gómez, A. Baxter, A. Cadden, and R. Berg, *Geotechnical Engineering Circular No. 7 Soil Nail Walls—Reference Manual*, U.S. Department of Transportation Publication No. FHWA-NHI-14-007, Federal Highway Administration (FHWA), Washington, DC, USA, 2015.

[2] I. Juran and V. Elias, *Soil Nailed Retaining Structures: Analysis of Case Histories*, Geotechnical Special Publication No. 12, ASCE, New York, NY, USA, 1987.

[3] I. Juran, G. Baudrand, K. Farrag, and V. Elias, "Kinematical limit analysis for design of soil-nailed structures," *Journal of Geotechnical Engineering*, vol. 116, no. 1, pp. 54–72, 1990.

[4] C. A. Lazarte, *Proposed Specifications for LRFD Soil-Nailing Design and Construction*, NCHRP Report 701, Transportation Research Board, National Research Council, Washington, DC, USA, 2011.

[5] C. A. Lazarte, V. Elias, D. Espinoza, and P. J. Sabatini, *Geotechnical Engineering Circular No. 7 Soil Nail Walls*, U.S. Department of Transportation Publication No. FHWA0-IF-03-017, Federal Highway Administration (FHWA), Washington, DC, USA, 2003.

[6] P. Lin, R. J. Bathurst, and J. Liu, "Statistical evaluation of the FHWA simplified method and modifications for predicting soil nail loads," *Journal of Geotechnical and Geoenvironmental Engineering*, vol. 143, no. 3, article 04016107, 2017b.

[7] K. K. Phoon and F. H. Kulhawy, "Characterization of model uncertainties for laterally loaded rigid drilled shafts," *Géotechnique*, vol. 55, no. 1, pp. 45–54, 2005.

[8] K. K. Phoon and C. Tang, "Model uncertainty for the capacity of strip footings under positive combined loading," in *Proceedings of Geotechnical Safety and Reliability: Honoring Wilson H. Tang (GSP 286)*, J. Huang, G. A. Fenton, L. Zhang, and D. V. Griffiths, Eds., pp. 40–60, ASCE, Reston, VA, USA, June 2017.

[9] C. Tang and K. K. Phoon, "Model uncertainty of cylindrical shear method for calculating the uplift capacity of helical anchors in clay," *Engineering Geology*, vol. 207, pp. 14–23, 2016.

[10] P. Lin, R. J. Bathurst, S. Javankhoshdel, and J. Liu, "Statistical analysis of the effective stress method and modifications for prediction of ultimate bond strength of soil nails," *Acta Geotechnica*, vol. 12, no. 1, pp. 171–182, 2017a.

[11] R. J. Bathurst, T. M. Allen, and A. S. Nowak, "Calibration concepts for load and resistance factor design (LRFD) of reinforced soil walls," *Canadian Geotechnical Journal*, vol. 45, no. 10, pp. 1377–1392, 2008.

[12] T. M. Allen and R. J. Bathurst, "Improved simplified method for prediction of loads in reinforced soil walls," *Journal of Geotechnical and Geoenvironmental Engineering*, vol. 141, no. 11, article 04015049, 2015.

[13] Y. Yu and R. J. Bathurst, "Analysis of soil-steel bar mat pullout models using a statistical approach," *Journal of Geotechnical and Geoenvironmental Engineering*, vol. 141, no. 5, article 04015006, 2015.

[14] D. M. Zhang, K. K. Phoon, H. W. Huang, and Q. F. Hu, "Characterization of model uncertainty for cantilever deflections in undrained clay," *Journal of Geotechnical and Geoenvironmental Engineering*, vol. 141, no. 1, article 04014088, 2015.

[15] International Organization for Standardization, *General Principles on Reliability of Structures*, ISO2394, Geneva, Switzerland, 2015.

[16] K. K. Phoon, "Role of reliability calculations in geotechnical design," *Georisk: Assessment and Management of Risk for Engineered Systems and Geohazards*, vol. 11, no. 1, pp. 4–21, 2017.

[17] P. Lin and R. J. Bathurst, "Influence of cross-correlation between nominal load and resistance on reliability-based design for simple linear soil-structure limit states," *Canadian Geotechnical Journal*, vol. 55, no. 2, pp. 279–295, 2018.

[18] M. Dithinde, K. K. Phoon, J. Ching, L. M. Zhang, and J. V. Retief, "Statistical characterization of model uncertainty," in *Chapter 5, Reliability of Geotechnical Structures in ISO2394*, K. K. Phoon and J. V. Retief, Eds., pp. 127–158, CRC Press/Balkema, Boca Raton, FL, USA, 2016.

[19] R. J. Byrne, D. Cotton, J. Porterfield, C. Wolschlag, and G. Ueblacker, *Manual for Design and Construction Monitoring of Soil Nail Wall*, U.S. Department of Transportation Publication No. FHWA-SA-96-069R, Federal Highway Administration (FHWA), Washington, DC, USA, 1998.

[20] AASHTO, *AASHTO LRFD Bridge Design Specifications*, AASHTO, Washington, DC, USA, 7th edition, 2014.

[21] FHWA, *Design and Construction of Mechanically Stabilized Earth Walls and Reinforced Soil Slopes—Volume I*, FHWA-NHI-10-024, FHWA GEC 011-Vol I, Federal Highway Administration (FHWA), Washington, DC, USA, 2009.

[22] S. Banerjee, A. Finney, T. D. Wentworth, and M. Bahiradhan, "Evaluation of design methodologies for soil-nailed walls," in *Volume 2: Distribution of Axial Forces in Soil Nails Based on Interpolation of Measured Strains*, Washington State Department of Transportation (WA-RD 371.2), Olympia, WC, USA, 1998.

[23] C. K. Shen, S. Bang, J. M. Romstad, L. Kulchin, and J. S. Denatale, "Field measurement of an earth support system," *Journal of the Geotechnical Engineering Division*, vol. 107, no. GT12, pp. 1625–1642, 1981.

[24] T. Holman and T. Tuozzolo, "Load development in soil nails from a strain-gauge instrumented wall," in *Proceedings of 2009 International Foundation Congress and Equipment Expo Contemporary Topics in Ground Modification, Problem Soils, and Geo-Support*, pp. 25–32, Orlando, FL, USA, March 2009.

[25] Y. Q. Wei, *Development of equivalent surcharge loads for the design of soil nailed segment of MSE/Soil nail hybrid retaining walls based on results from full-scale wall instrumentation and finite element analysis*, Ph.D. thesis, Texas Tech University, Lubbock, TX, USA, 2013.

[26] M. J. Zhang and Z. X. Guo, "Research on behaviors of soil nailing by field test," *Chinese Journal of Geotechnical Engineering*, vol. 23, no. 3, pp. 319–323, 2001, in Chinese.

[27] J. L. Duan, Y. H. Tan, Y. W. Fan, and F. Lu, "Field testing study on composite soil nailing," *Chinese Journal of Mechanical Engineering*, vol. 23, no. 12, pp. 2128–2132, 2004, in Chinese.

[28] G. H. Yang, "Calculation of soil nail forces and displacement in soil nailing retaining wall," *Rock and Soil Mechanics*, vol. 33, no. 1, pp. 137–146, 2012, in Chinese.

[29] J. Cao, M. G. Xiao, and X. H. Xu, "Estimating of the axial nailing stress in soil nailed walls," *Soils and Foundations*, vol. 27, no. 3, pp. 80–82, 2013, in Chinese.

[30] A. N. Liu, Q. Z. Lai, R. G. Wu, and C. Y. Su, "Monitoring and analysis of soil nail axial force on the upper part of a soil nail wall for the deep foundation," *Journal of Sichuan University (Natural Science Edition)*, vol. 28, no. 1, pp. 59–62, 2015, in Chinese.

[31] S. G. Wang, Q. W. Duan, and Y. Y. Wang, "Research on the soil nail wall by field tests," *Building Science*, vol. 26, no. 1, pp. 90–92, 2010, in Chinese.

[32] A. Sawicki, D. Lesniwwska, and M. Kulczykowski, "Measured and predicted stresses and bearing capacity of a full scale slope reinforced with nails," *Soils and Foundations*, vol. 28, no. 4, pp. 47–56, 1998.

[33] J. P. Turner and W. G. Jensen, "Landslide stabilization using soil nail and mechanically stabilized earth walls: case study," *Journal of Geotechnical and Geoenvironmental Engineering*, vol. 131, no. 2, pp. 141–150, 2005.

[34] S. W. Jacobsz and T. S. Phalanndwa, "Observed axial loads in soil nails," in *Proceedings of 15th African Regional Conference on Soil Mechanics and Geotechnical Engineering*, Maputo, Mozambique, July 2011.

[35] B. M. Das, *Principles of Foundation Engineering*, Cengage Learning, Boston, MA, USA, 2018.

[36] D. Kim and R. Salgado, "Load and resistance factors for external stability checks of mechanically stabilized earth walls," *Journal of Geotechnical and Geoenvironmental Engineering*, vol. 138, no. 3, pp. 241–251, 2012a.

[37] D. Kim and R. Salgado, "Load and resistance factors for internal stability checks of mechanically stabilized earth walls," *Journal of Geotechnical and Geoenvironmental Engineering*, vol. 138, no. 8, pp. 910–921, 2012b.

[38] P. Lin, J. Liu, and X. Yuan, "Reliability analysis of soil nail walls against external failures in layered ground," *Journal of Geotechnical and Geoenvironmental Engineering*, vol. 143, no. 1, article 04016077, 2017d.

[39] Y. Wang, Z. Cao, and D. Li, "Bayesian perspective on geotechnical variability and site characterization," *Engineering Geology*, vol. 203, pp. 117–125, 2016.

[40] L. Zhang, D. Q. Li, X. S. Tang, Z. J. Cao, and K. K. Phoon, "Bayesian model comparison and characterization of bivariate distribution for shear strength parameters of soil," *Computers and Geotechnics*, vol. 95, pp. 110–118, 2018.

[41] W. H. Zhou, F. Tan, and K. V. Yuen, "Model updating and uncertainty analysis for creep behavior of soft soil," *Computers and Geotechnics*, vol. 100, pp. 135–143, 2018.